ANALYTICAL AND NUMERICAL STUDIES FOR THE REDUCTION OF WAVE RUN-UP HEIGHT BY A SUBMERGED BREAKWATER

*Ikha Magdalena¹, Josephine Listya Elfandana Suhardi¹ and Mohammad Bagus Adityawan²

¹Faculty of Mathematics and Natural Sciences, Bandung Institute of Technology, Indonesia; ² Faculty of Civil and Environmental Engineering, Bandung Institute of Technology, Indonesia

*Corresponding Author, Received: 08 July 2020, Revised: 01 Sep. 2020, Accepted: 24 Oct. 2020

ABSTRACT: Submerged breakwaters are designed to reduce the wave run-up in coastal areas. The effectiveness can be modelled using numerical methods. The Nonlinear Shallow Water Equation has been applied as the fundamental model. The equation has been solved analytically and numerically to obtain the run-up coefficient. The results from the analytical and numerical solutions have been combined with published experimental data to validate the analytical model and numerical scheme. It is found that both analytical and numerical results are in a very good agreement with the experimental data with relatively small errors. Furthermore, the numerical scheme has been implemented to observe the influence of the breakwater's characteristics, such as its height and length, towards the reduction of wave run-up. From the observation, the optimum size of the breakwater is determined to reduce the wave run-up as much as possible. The results can be applied to future design of submerged breakwaters for reducing long wave run-up.

Keywords: Submerged breakwater; Run-up; Nonlinear Shallow Water Equation

1. INTRODUCTION

One of the most dangerous disasters in coastal areas is tsunami. For example, the Indian Ocean tsunami in 2014 and the Japan tsunami in 2011 wiped out almost everything in vicinity. Several researchers have studied the impact of tsunami such as in [1-3]. They analyzed the bathymetric data before and after the tsunami using the rapid visual method. From these unfortunate disasters, the cause of tsunami wave has been studied using experimental and analytical methods such as in [4-9]. Many researchers have done other studies about wave run-up using mathematical models, such as [10-14]. One of the ways to diminish the severity of wave run-up is to lower the amplitude of the incoming waves. There are several methods to reduce the wave amplitude; one of them is using the submerged breakwater. Some researchers have studied about the submerged breakwater experimentally such as [15,16]. However. experimental approach is costly, subject to high overheads, and impractical. Consequently, other researchers attempted to use mathematical models to study breakwater as in [17-25]. Their present studies have suggested that submerged breakwater can reduce the wave amplitude. Nevertheless, the majority of those studies utilise potential theory or mild slope equations which are relatively difficult to be solved analytically and numerically. In another study, Fatemeh [26] discusses the effect of the submerged breakwater on wave energy dissipation. The model is based on RANS equation inclosure with a standard k-€ turbulence model. However, this method also has several challenges which are the lengthy computational time and its complicated derivatives.

In addition to all of the shortcomings above, it is also not yet known the effect of submerged breakwater towards wave run-up reduction. Therefore, in this research, the effectiveness of a rectangular submerged breakwater to minimize wave run-up will be investigated through a mathematical model, the Non-Linear Shallow Water Equation. This model will be solved analytically obtain maximum wave run-up. Then, the numerical scheme used will be derived by the finite volume on a staggered grid method that is free from damping error [27-32]. The nonlinear mathematical model was evaluated by comparing with the results from [33], they evaluated the evolution of nonlinear long waves in convergingdiverging channels of variable depth and width. Furthermore, the numerical scheme obtained will be compared with the experimental data from [34,11]. In the end, the results of the simulation will be able to determine the effectiveness of submerged breakwater to wave run-up reduction.

2. MATHEMATICAL MODEL

In this research, the authors observed a domain with a rectangular submerged breakwater over a flat bottom and a single sloping beach. The incoming waves propagate from the sea towards the coast over the breakwater and approach the sloping beach. Furthermore, the vertical height above the

still-water level along the beach or also known as the wave run-up is measured.

First, the observation domain is divided into four regions: Ω_1 , Ω_2 , Ω_3 , and Ω_4 , where Ω_1 and Ω_3 have flat bottom topography, Ω_2 has a rectangular breakwater over a flat bottom topography, and Ω_4 has the sloping beach bottom topography (see Fig. 1). Hence, the depth function is described as follows:

$$d(x) = \begin{cases} h_0, & if \quad x \in \Omega_1 \\ h_1, & if \quad x \in \Omega_2 \\ h_0, & if \quad x \in \Omega_3 \\ \alpha x, & if \quad x \in \Omega_4 \end{cases}$$
 (1)

where h_0 is a positive constant representing the water depth in Ω_1, Ω_3 , h_1 is water depth that is measured from the peak of the breakwater to the still water level, and α is the angle of the slope.

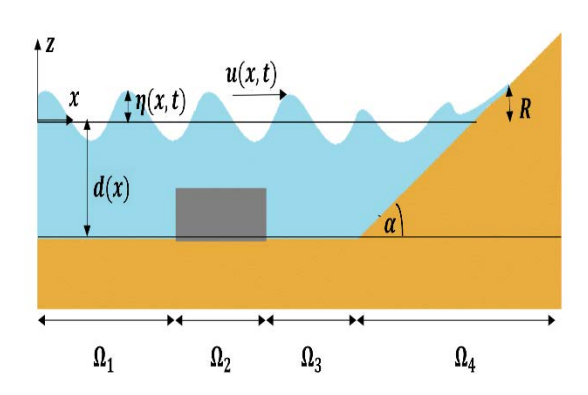


Fig.1 Problem sketch for mathematical model

Here, the Non-Linear Shallow Water Equations (NSWE) is used to study the reduction of the wave run-up by the submerged breakwater. Let $\eta(x,t)$ and u(x,t) denote surface elevation and average horizontal velocity, respectively. Notation g is for the gravitational acceleration. The water thickness is defined by $h(x,t) = \eta(x,t) + d(x)$, with d(x) is the water depth measured from the still water level. Therefore, the NSWE reads as:

$$\eta_t + (hu)_x = 0, \tag{2}$$

$$u_t + uu_x + g\eta_x = 0. (3)$$

where Eq. (2) and Eq. (3) represent the mass conservation and momentum balance equation, respectively.

3. ANALYTICAL SOLUTION

In this section, an analytical solution will be derived from the Linearized-SWE to obtain the maximum height of wave run-up. Assuming that the

surface elevation is relatively small compared to the water depth $\eta << d$, thus h = d, yields in:

$$\eta_t + (du)_x = 0, \tag{4}$$

$$u_t + g\eta_x = 0. (5)$$

The analytical solution for surface elevation and horizontal velocity will be derived in each of the four domains, according to the following problem sketch:

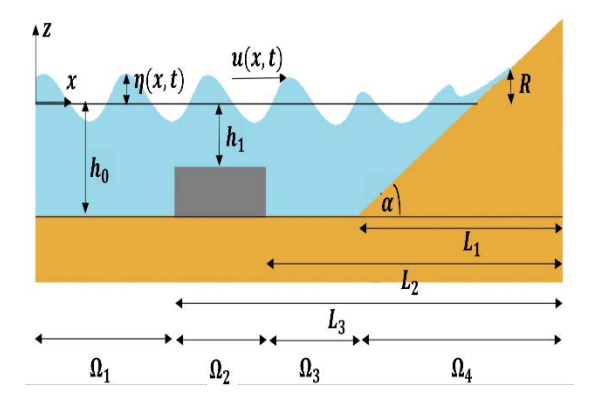


Fig.2 Domain description for deriving the analytical solution

Here, the authors use variable separation method by assuming the incoming wave is a monochromatic wave with a certain frequency (ω) . $\eta(x,t)$ and u(x,t) can be written as follows:

$$\eta(x,t) = F(x)e^{-i\omega t},\tag{6}$$

$$u(x,t) = G(x)e^{-i\omega t}. (7)$$

First, the analytical solution at the domain Ω_1 will be derived. Consider the following equations:

$$\eta_1(x,t) = F_1(x)e^{-i\omega t},\tag{8}$$

$$\mathbf{u}_{1}(\mathbf{x},t) = \mathbf{G}_{1}(\mathbf{x})e^{-i\omega t}.\tag{9}$$

By substituting Eq. (8) and (9) to the mass conservation equation (see Eq. (4)) and momentum balance equation (see Eq. (5)), the following equations are obtained:

$$F_1(x) = \frac{h_0}{i\omega} G_1'(x), \tag{10}$$

$$G_1(x) = \frac{g}{i\omega} F_1'(x).$$
 (11)

Differentiate Eq. (11) with respect to x,

$$G_1'(x) = \frac{g}{i\omega} F_1''(x).$$
 (12)

Substituted Eq. (11) to Eq. (10) results in the following ordinary second order differential equation:

$$F_1''(x) + \frac{w^2}{gh_0}F_1(x) = \mathbf{0},\tag{13}$$

where h_0 denotes the water depth at Ω_1 . The solution of Eq. (13) is

$$F_1(x) = A_i e^{\left(\frac{w}{\sqrt{gh_0}}ix\right)} + A_r e^{\left(-\frac{w}{\sqrt{gh_0}}ix\right)}.$$
 (14)

where A_i is the amplitude of the incoming wave and A_r is the amplitude of the reflection wave. Thus, the analytical solution for wave elevation at Ω_1 is

$$\eta_1(x,t) = A_i e^{\left(\frac{w}{\sqrt{gh_0}}x - \omega t\right)i} + A_r e^{\left(-\frac{w}{\sqrt{gh_0}}x - \omega t\right)i}. \quad (15)$$

Next, by using the same technique, the solution for surface elevation in domain Ω_2 is as follow:

$$\eta_2(x,t) = ae^{(\frac{w}{\sqrt{gh_1}}x - \omega t)i} + be^{(-\frac{w}{\sqrt{gh_1}}x - \omega t)i}.$$
 (16)

Moving right along, the analytical solutions for domain Ω_3 will be derived using the same techniques as the calculations in domain Ω_1 . Thus, the analytical solution for wave elevation at Ω_3 is:

$$\eta_3(x,t) = B_i e^{(\frac{w}{\sqrt{gh_0}}x - \omega t)i} + B_r e^{(-\frac{w}{\sqrt{gh_0}}x - \omega t)i}, \quad (17)$$

where h_0 denotes the water depth at Ω_1 and Ω_3 .

Lastly, in order to get the analytical solution in domain Ω_4 , note that the depth of water in the domain Ω_4 is expressed by $d(x) = \alpha x$. Hence, the shallow water equation can be expressed as:

$$\eta_t + ((d+\eta)u)_x = 0, \tag{18}$$

$$u_t + g\eta_x = 0. (19)$$

Eq. (18) and Eq. (19) can be simplified to:

$$(\boldsymbol{\eta}_t)_t - \boldsymbol{g}(\boldsymbol{d}\boldsymbol{\eta}_x)_x = \mathbf{0}. \tag{20}$$

Then, $\eta_4(x, t)$ can be stated as:

$$\eta_4(x,t) = A(x)e^{-i\omega t}. (21)$$

Substitute the Eq. (21) to the Eq. (20), yields in:

$$g\alpha(x(A_r)_r + A_r) + \omega^2 A = 0. \tag{22}$$

The solution of the Eq. (20) contains the Bessel function as follow:

$$A(x) = C_1 J_0(\sqrt{\frac{4\omega^2 x}{g\alpha}}) + C_2 Y_0(\sqrt{\frac{4\omega^2 x}{g\alpha}}).$$
 (23)

At the shore, the amplitude value is finite and given that $Y_0(\sqrt{\frac{4\omega^2x}{g\alpha}}) \neq 0$, hence $C_2 = 0$. Therefore, the solution of Eq. (23) is:

$$\eta_4(x,t) = C_1 J_0(\sqrt{\frac{4\omega^2 x}{g\alpha}}) e^{-iwt}. \tag{24}$$

Moreover, at the shore, $\eta_4(0,t) = C_1 e^{-iwt}$ with C_1 as the maximum value. Hence, C_1 is the maximum run-up height which will be denoted by R. Thus Eq. (24) can be written as:

$$\eta_4(x,t) = RJ_0(\sqrt{\frac{4\omega^2x}{g\alpha}})e^{-iwt}.$$
 (25)

Then, since continuity condition for η and $\frac{\partial \eta}{\partial x}$ have to be satisfied at $x = L_1$, $x = L_2$, and $x = L_3$, the following systems of equations are obtained:

• At $x = L_1$,

$$RJ_0(\gamma_1) = B_i e^{\gamma_2} + B_r e^{-\gamma_2}, \tag{26}$$

$$Ri\sqrt{\frac{h_0}{\alpha L_1}}J_1(\gamma_1) = B_i e^{\gamma_2} - B_r e^{-\gamma_2}.$$
 (27)

From Eq. (26) and Eq. (27),

$$\boldsymbol{B}_{i} = \boldsymbol{R}.\boldsymbol{P},\tag{28}$$

$$\boldsymbol{B_r} = \boldsymbol{R}.\boldsymbol{Q},\tag{29}$$

$$P = \frac{J_0(\gamma_1) + i\sqrt{\frac{h_0}{aL_1}}J_1(\gamma_1)}{2e^{\gamma_2}} \text{ and } Q = \frac{J_0(\gamma_1) - i\sqrt{\frac{h_0}{aL_1}}J_1(\gamma_1)}{2e^{-\gamma_2}}.$$

• At $x = L_2$,

$$B_i e^{\gamma_3} + B_r e^{-\gamma_3} = a e^{\gamma_4} + b e^{-\gamma_4},$$
 (30)

$$\sqrt{\frac{h_1}{h_0}} (B_i e^{\gamma_3} - B_r e^{-\gamma_3}) = a e^{\gamma_4} - b e^{-\gamma_4}.$$
 (31)

From Eq. (30) and Eq. (31),

$$a = R.M, (32)$$

$$\boldsymbol{b} = \boldsymbol{R}.\boldsymbol{N},\tag{33}$$

$$b = R. N,$$
with $M = \frac{(1 + \sqrt{\frac{h_1}{h_0}})Pe^{\gamma_3} + (1 - \sqrt{\frac{h_1}{h_0}})Qe^{-\gamma_3}}{2e^{\gamma_4}}$ and $N = \frac{(1 - \sqrt{\frac{h_1}{h_0}})Pe^{\gamma_3} + (1 + \sqrt{\frac{h_1}{h_0}})Qe^{-\gamma_3}}{2e^{-\gamma_4}}$.

• At $x = L_3$

$$ae^{\gamma_5} + be^{-\gamma_5} = A_i e^{\gamma_6} + A_r e^{-\gamma_6},$$
 (34)

$$\sqrt{\frac{h_0}{h_1}}(ae^{\gamma_5} - be^{-\gamma_5}) = A_i e^{\gamma_6} - A_r e^{-\gamma_6}.$$
 (35)

From Eq. (34) and (35),

$$\frac{R}{A_i} = \frac{1}{U'} \tag{36}$$

with
$$U = \frac{(1+\sqrt{\frac{h_0}{h_1}})Me^{\gamma_5} + (1-\sqrt{\frac{h_0}{h_1}})Ne^{-\gamma_5}}{2e^{\gamma_6}}$$
.

The Eq. (36) will be referred as the run-up coefficient.

4. NUMERICAL METHOD

In this section, the numerical scheme will be derived. Here, the finite volume on a staggered grid method is used, as illustrated in Fig. 3. Suppose the length of the observation domain is [0, L]. The domain is partitioned in a staggered way into half and full grids with a spatial step Δx .

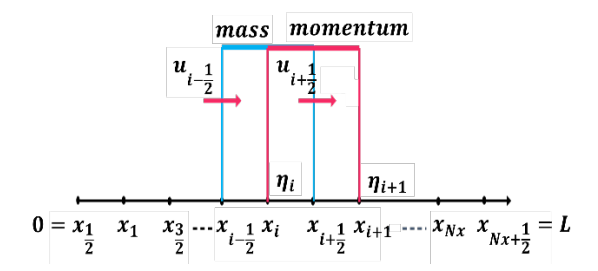


Fig.3 Staggered grid illustration

Equation (2) will be calculated in cells $[x_{j-\frac{1}{2}}, x_{j+\frac{1}{2}}]$ or cells with blue line, while Eq. (3) will be calculated in cells $[x_j, x_{j+1}]$ or cells with red line. Here, the wave elevation $\eta(x, t)$ and h(x, t) are calculated at the point with the full grid x_j , while u is calculated at every half-grid point $x_{j+\frac{1}{2}}$. Using Forward Time Centered Space, the numerical approximation of Eq. (2) and Eq. (3) are:

$$\frac{\eta_j^{n+1} - \eta_j^n}{\Lambda t} + \frac{(hu)_{j+\frac{1}{2}}^n - (hu)_{j-\frac{1}{2}}^n}{\Lambda x} = \mathbf{0},\tag{37}$$

$$\frac{u_{j+\frac{1}{2}-j+\frac{1}{2}}^{n-1}}{\Delta t} + g \frac{\eta_{j+1}^{n+1} - \eta_{j}^{n+1}}{\Delta x} + (uu_{x})_{j+\frac{1}{2}}^{n} = \mathbf{0},$$
 (38)

where subscripts and superscripts denote the spatial grid point and time, respectively. Note that h does not have a value in the half-grid point to calculate

hu. Therefore, **h** will be approximated using the first-order upwind scheme which depends on the flow velocity. A new **h** is denoted with the symbol ***h** described as follow:

$${}^{*}h_{j+\frac{1}{2}}^{n} = \begin{cases} h_{j}^{n}, & if \quad u_{j+\frac{1}{2}}^{n} > 0\\ h_{j+1}^{n}, & if \quad u_{j+\frac{1}{2}}^{n} < 0 \end{cases}$$
(39)

Then, one of the challenges on solving NSWE numerically is to approximate the advection term which is denoted by uu_x . Here, a simple method is proposed to approximate the uu_x . First, write the following equation:

$$uu_x = \frac{qu_x}{h} = \frac{q}{h} \frac{\partial u}{\partial x},\tag{40}$$

with $\mathbf{q} = \mathbf{h}\mathbf{u}$. Next, Eq. (40) can be written as

$$(uu_{x})_{j+\frac{1}{2}} = \frac{\overline{q}_{j+\frac{1}{2}}}{\overline{h}_{j+\frac{1}{2}}} {\binom{*u_{j+1} - *u_{j}}{\Delta x}}, \tag{41}$$

where

$$\overline{h}_{j+\frac{1}{2}} = \frac{1}{2}(h_j + h_{j+1}),$$
 (42)

$$\overline{q}_{j} = \frac{1}{2} (q_{j+\frac{1}{2}} + q_{j-\frac{1}{2}}), \tag{43}$$

$$q_{j+\frac{1}{2}} = h_{j+\frac{1}{2}} u_{j+\frac{1}{2}}. \tag{44}$$

The value of *u_j is approximated with the first-order upwind scheme as follow:

$${}^{*}u_{j+\frac{1}{2}}^{n} = \begin{cases} u_{j-\frac{1}{2}}, & if \quad \overline{q}_{j} \ge 0 \\ u_{j+\frac{1}{2}}, & if \quad \overline{q}_{j} < 0 \end{cases}$$
(45)

In order to simulate the wave propagation over a sloping structure h, it is necessary for the numerical scheme to adapt with the moving wet-dry interface. Therefore, the discrete formula for Eq. (38) will be computed only if the water depth is greater than a minimum threshold depth h = 0.

5. RESULTS AND DISCUSSIONS

In this section, the numerical scheme will be implemented. Several simulations are presented to study the reduction of the amplitude by the submerged breakwater. For validation, first, the numerical results will be compared with the experimental data from [34] to observe its ability to simulate the wave run-up over a sloping bottom. Second, the capability of the numerical scheme to

simulate the wave run-up over a submerged breakwater and a sloping bottom will be confirmed. For this part, it will be compared with the analytical solution that has been obtained in Section 3 and also with the experimental data from [11]. After the numerical scheme has been examined, the effect of the breakwater's characteristic on the wave run-up will be investigated further.

5.1 Wave Run-up over a Sloping Bottom

Here, the accuracy of the numerical scheme to simulate the wave run-up over a sloping bottom will be examined. The numerical results will be validated by comparing with the experimental data in [34]. The initial conditions and parameters used in numerical simulation will be determined according to the experiment setup.

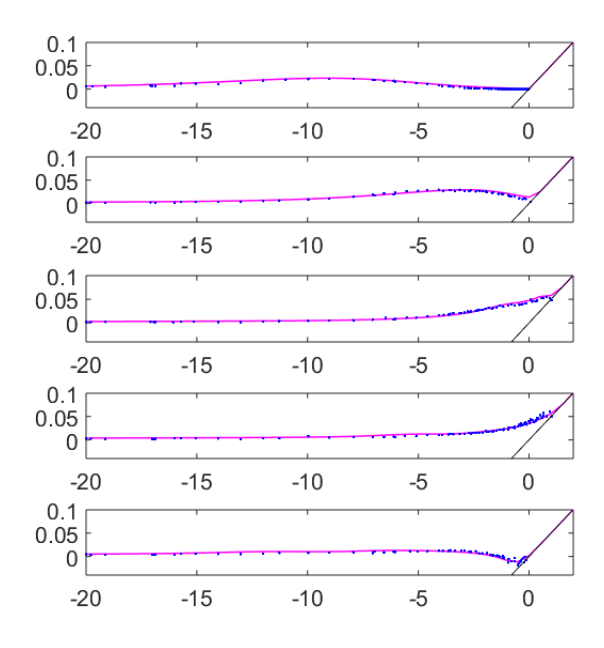


Fig.4 Wave surfaces at T = 30, 40, 50, 60, 70 s

The Synolakis' experiment was done in 31.73 cm length, 39.97 cm width, and 60.96 cm depth wave tank. The waves first propagate from a position of L_g from the edge of slope beach with $L_g = \frac{1}{\gamma} \arccos \sqrt{20}$. The slope angle used is 1/19.85. Consider the following initial condition:

$$\eta(x,0) = Asech^2(\gamma(x-x_0)) \tag{46}$$

with

$$u_1(x,0) = \eta(x,0) \sqrt{\frac{g}{H'}}$$
 (47)

where notation A is the wave amplitude, H is the depth of water in the constant domain, g is the acceleration of gravity, x_0 is the position of the wave crest, and $\gamma = \sqrt{\frac{3A}{4d_0}}$. This initial condition produces a solitary wave propagating towards the sloping beach on the right. The parameters used in this simulation are g=1 and $d_0=1$. To avoid the breaking wave phenomenon, A=0.0185 and $x_0=38.34$ are chosen.

Figure 4 shows that the surface elevation from the numerical simulations (denoted by the solid line) confirm the experimental data (indicated by the dashed line) at five different times $T = 30,40,50,60,70 \, s$. This finding implies that the numerical scheme is able to simulate wave run-up with a moving boundary accurately. In this particular test case, the wet-dry procedure plays an important role to produce results correctly.

5.2 Wave Run-up over a Submerged Breakwater and a Sloping Bottom

In this sub-section, the ability of the numerical scheme to simulate the wave run-up over a submerged breakwater and a sloping bottom will be validated. First, the numerical results will be compared with the analytical solution. Next, the result from the numerical scheme will also be validated with the experimental data from [11].

5.2.1 Comparison between numerical and analytical result

First, simulations were carried out with various sizes of breakwaters using the following initial condition:

$$\eta = Asin(wt) \tag{48}$$

The values used in Figure 2 are $h_0 = 0.8$ m, h_1 varies between 0.3-0.5 m, $\alpha = 1/2$, and $L_1 = 2.5$ m, $L_2 = 4$ m, and L_3 varies between 5-10 m. In addition, $\omega = 0.3\pi$ rad/s is used with the observation duration T = 30 s. The comparison between the non-dimensional run-up coefficient (R/Am) resulting from the numerical simulation and analytical solution is presented in the Table 1.

From the table above, it can be seen that the runup coefficients from the numerical simulation confirm the analytical results with the RMSE value is 0.052.

5.2.2 Comparison between numerical and experimental results

Shing Tony's [11] experiment was done in 1.25 feet (0.38 m) length, 6 inches (0.15 m) width, and 3/16 inches (0.0048 m) depth wave tank, and 5

degrees slope. The ratio between breakwater height and depth of water is 3:10. There are four width variations of the breakwater: 30 inches (0.76 m), 60 inches (1.52 m), 90 inches (2.29 m), and 120 inches (3.05 m). Here, a solitary wave is simulated with the following initial and boundary condition:

$$\eta(0,t) = \frac{\alpha^2(kx - kx_0)}{1 - \alpha \tanh^2(kx - kx_0)}$$
 (49)

Table 1 Comparison between numerical and analytical run-up coefficient

Am (m)	h ₁ (m)	L ₃ (m)	Analytical R/Am	Numerical R/Am
.02	0.3	5	2.396	2.400
.045	0.3	6	2.531	2.555
.016	0.3	7	3.171	3.125
.026	0.3	8	3.892	3.846
.012	0.3	9	3.292	3.333
.2	0.3	10	2.585	2.525
.016	0.4	5	2.517	2.500
.0155	0.4	6	2.588	2.500
.025	0.4	7	2.942	3.000
.032	0.4	8	3.433	3.438
.207	0.4	9	3.470	3.382
.021	0.4	10	2.993	2.976
.03	0.5	5	2.597	2.620
.03	0.5	6	2.636	2.580
.04	0.5	7	2.839	2.750
.032	0.5	8	3.129	3.125
.03	0.5	9	3.277	3.333
.022	0.5	10	3.113	3.181

$$u(x,0) = \sqrt{\frac{g}{H}} \eta(x,0)$$
 (50)

with

$$k = \sqrt{\frac{3\alpha}{4(1+0.068\alpha)}} \tag{51}$$

Table 2 Experimental and numerical run-up without breakwater

Am	Analytical	Numerical	Error
(m)	R/Am	R/Am	
.0320	0.0460	0.0459	0.2174
.0630	0.1010	0.0934	7.5248
.0750	0.1380	0.1385	0.3623
.1170	0.1580	0.1578	0.1266
.1270	0.1900	0.1900	0.0000
.1480	0.2500	0.2491	0.3600
.1740	0.3200	0.3203	0.0937
.2070	0.3630	0.3633	0.0826

.2330	0.4050	0.4053	0.0741
.2580	0.4610	0.4607	0.0651

Table 3 Experimental and numerical run-up with 30 inches breakwater

Am	Analytical	Numerical	Error
(m)	R/Am	R/Am	
.0180	0.0360	0.0359	0.2778
.0550	0.0730	0.0720	1.3699
.0880	0.1150	0.1171	1.8261
.1050	0.1560	0.1562	0.1282
.1240	0.1920	0.1921	0.0521
.1370	0.2430	0.2427	0.1235
.1750	0.3050	0.3047	0.0984
.2070	0.3680	0.3681	0.0272
.2180	0.3990	0.3989	0.0251
.2500	0.4510	0.4504	0.1330

Table 4 Experimental and numerical run-up with 60 inches breakwater

Am	Analytical	Numerical	Error
(m)	R/Am	R/Am	
.0190	0.0260	0.0259	0.3846
.0570	0.0600	0.0602	0.3333
.0770	0.1220	0.1227	0.5738
.1070	0.1490	0.1499	0.6040
.1210	0.1760	0.1765	0.2841
.1320	0.2130	0.2135	0.2347
.1620	0.2650	0.2660	0.3774
.1880	0.3110	0.3113	0.0965
.2100	0.3420	0.3419	0.0292
.2450	0.4050	0.4021	0.7160

Table 5 Experimental and numerical run-up with 90 inches breakwater

Am	Analytical	Numerical	Error
(m)	R/Am	R/Am	Litor
.0200	0.0290	0.0285	1.7241
.0630	0.0790	0.0781	1.1392
.0710	0.1160	0.1171	0.9483
.1100	0.1490	0.1499	0.6040
.1230	0.1910	0.1908	0.1047
.1390	0.2360	0.2367	0.2966
.1640	0.2680	0.2681	0.0373
.2080	0.3470	0.3472	0.0576
.2290	0.3830	0.3831	0.0261
.2570	0.4120	0.4116	0.0971

From Table 2 – Table 6, it can be seen that the relative errors are very small, which implies that the numerical scheme is able to simulate the wave runup over a sloping bottom, both with and without the existence of submerged breakwater. Furthermore, it signifies that the submerged breakwater is able to reduce the height of wave run-up. However, further analysis is needed to observe the influence of the length of breakwater towards the reduction of wave run-up, which will be discussed in the next section.

Table 6 Experimental and numerical run-up with 120 inches breakwater

Am	Analytical	Numerical	Error
(m)	R/Am	R/Am	
.0400	0.0310	0.0309	0.3226
.0480	0.0550	0.0554	0.7273
.0830	0.1120	0.1171	4.5536
.1190	0.1610	0.1615	0.3106
.1260	0.1770	0.1755	0.8475
.1430	0.2540	0.2533	0.2756
.1750	0.2940	0.2968	0.9524
.2000	0.3190	0.3193	0.0940
.2300	0.4090	0.4090	0.0000
.2570	0.4230	0.4235	0.1182

5.3 Sensitivity Analysis

After the numerical scheme is confirmed, this section will discuss on how to use it to analyze the optimal breakwater size to minimize the height of wave run-up. From Figure 5, for every h_1 value, the run-up reduction tends to oscillate as the length of the breakwater continues to increase. Here, notation h_1 is the depth of water calculated from the top of breakwater to shallow water, d is the depth of shallow water, and L_b is the length of breakwater.

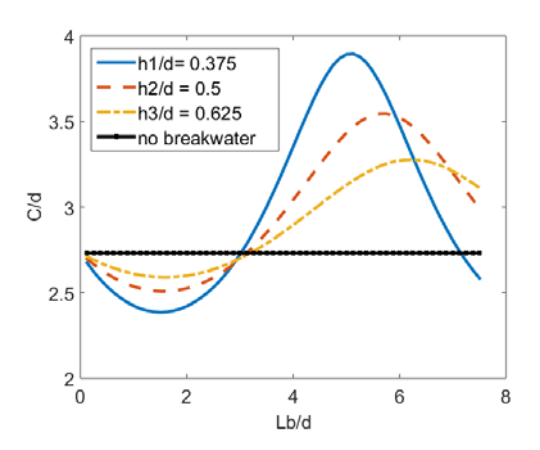


Fig.5 R/Am against the length of the breakwater

Breakwaters are said to be effective if the runup coefficient is below the black constant line. While a breakwater is said to be optimal if the runup coefficient has the smallest value of the other breakwaters. The most optimal value of h_1 in this case is $h_1/d = 0.375$ and the optimal breakwaters length are Lb/d = 1.45. To determine the optimal breakwater length due to the oscillate result, the shortest length can be chosen. This way, the installation costs will be minimized. Therefore, h_1 = 0.3 m is chosen, with the length of the breakwater is between 0.5-0.8 m as the optimal breakwater length setting for this case.

6. CONLUSIONS

In this paper, the authors have derived a numerical model that is able to simulate run-up waves after passing through submerged rectangular breakwater well. The analytical solution shows the reduction of the wave runup depends on the size of breakwater. Moreover, the numerical results show a good agreement with the analytical solution and experimental data from Shing Tony (2014). It is indicated by RMSE value that is approaching to zero and also the small value of relative errors. Subsequently, the length of the breakwater which gives the lowest run-up height has been determined using two methods. After varying the length of breakwater, the authors found that a breakwater with $h_1/d = 0.375$ and length between Lb/d =1.45 produces the lowest run-up coefficient and minimum estimated installation cost. The authors believe that the result from this research will be beneficial as a part of assessment tool to build a breakwater which aims to reduce the risk of wave run-up.

7. REFERENCES

- [1] Hagan A., Foster R., Perera N., Gunawan C., Silaban I., Yaha Y., Manuputty Y., Hazam I., and Hodgson G., Tsunami Impacts in Aceh Province and North Sumatra, Indonesia, Atoll Research Bulletin, Vol. 544, 2007, pp. 37–54.
- [2] Adityawan M., Dao N., Tanaka H., Mano A., and Udo K., Morphological Changes along the Ishinomaki Coast Induced by the 2011 Great East Japan Tsunami and the Relationship with Coastal Structures, Coastal Engineering Journal, Vol. 56, Issue 3, 2014, 1450016 (21 pages).
- [3] Sihombing Y., Adityawan M., Chrysanti A., Widyaningtias W., Farid M., Nugroho J., Adi Kuntoro A., and Kusuma M., Tsunami Overland Flow Characteristic and Its Effect on Palu Bay due to the Palu Tsunami 2018, Journal of Earthquake and Tsunami, Vol. 14, Issue 2, 2019, 2050009.

- [4] Madsen P. A., Fuhrman D. R., and Schaffer H. A., On the Solitary Wave Paradigm for Tsunamis, Journal of Geophysical Research: Oceans, Vol. 13, 2008, C12012 (22 pages).
- [5] Allsop W., Chandler I., and Zaccaria M., Improvements in the Physical Modelling of Tsunamis and Their Effects, in Proceeding CoastLab Conference, 2014, Varna, Bulgaria.
- [6] Esteban M., Glasbergen T., Takabatake T., Hofland B., Nishizaki S., Nishida Y., Stolle J., Nistor I., Bricker J., Takagi H., and Shibayama T., Overtopping of Coastal Structures by Tsunami Waves, Geosciences, Vol. 7, Issue 4, 2017, 121 (17 pages).
- [7] Goseberg N., Wurpts A., and Schlurmann T., Laboratory-scale Generation of Tsunami and Long Waves, Coastal Engineering, Vol. 79, 2013, pp. 57-74.
- [8] Schimmels S., Sriram V., Didenkulova I., and Fernandez H., On the Generation of Tsunami in a Large Scale Wave Flume, Coastal Engineering Proceedings, Vol. 1, Issue 34, 2014, 14.
- [9] Bricker J., Nakayama A., Takagi H., Mitsui J., and Miki T., Chapter 19: Mechanisms of Damage to Coastal Structures due to the 2011 Great East Japan Tsunami, Handbook of Coastal Disaster Mitigation for Engineers and Planners, Butterworth-Heinemann, 2015, pp. 385-415.
- [10] Mohandie R. and Teng M., Numerical and Experimental Study on Reducing Long Wave Run-up by Beach Vegetation, in Proceeding of the 21st International Offshore (Ocean) and Polar Engineering Conference, 2011.
- [11] Tony S. K., Experimental Study on the Effect of Submerged Breakwater Configuration on Long Wave Run-up Reduction, M.S. Thesis, Department of Civil and Environmental Engineering, University of Hawaii, 2014.
- [12] Irtem E., Seyfoglu E., and Kabdasli S., Experimental Investigation on the Effects on Submerged Breakwater on Tsunami Run-up Height, in Proceeding of the 11th International Coastal Symposium, Vol. 64, 2011, pp. 516– 520.
- [13] Shimabuku N., Long Wave Run-up over Submerged Reef and Breakwater, M.S. Thesis, Department of Civil and Environmental Engineering, University of Hawaii, 2012.
- [14] Lee J. and Liu C., A New Solution of Waves Passing a Submerged Porous Structure, in Proceeding of the 17th Ocean Engineering Conference, 1995, pp. 593–606.
- [15] Lokesha, Kerpen N. B., Sannasiraj S. A., Sundar V., and Schlurmann T., Experimental Investigations on Wave Transmission at Submerged Breakwater with Smooth and

- Stepped Slopes. in Proceeding of the 8th International Conference on Asian and Pacific Coasts, Vol. 116, 2015, pp.713-719.
- [16] Stamos D. G., Hajj M. R., and Telionis D. P., Performance of Hemi-cylindrical and Rectangular Submerged Breakwaters, Ocean Engineering, Vol. 30, Issue 6, 2003, pp. 813-828.
- [17] Rojanakamthorn S., Isobe M., and Watanabe A., A Mathematical Model of Wave Transformation over a Submerged Breakwater, Coastal Engineering in Japan, Vol. 32, 1989, pp. 209–234.
- [18] Abdul Khader M. I., and Rai S. P., A Study of Submerged Breakwater, Journal of Hydraulic Research, Vol. 18, Issue 2, 1980, pp. 113-121.
- [19] Dick T. M. and Brebner A., Solid and Permeable Breakwaters, in Proceeding 11th International Conference on Coastal Engineering Proceedings, Vol. 1, Issue 11, 1968, pp. 1141-1158.
- [20] Seabrook S. R. and Hall K. R., Wave Transmission at Submerged Rubblemound Breakwaters, Ocean Engineering, 1998, pp. 2000-2013.
- [21] Naftzger R. A. and Chakrabarti S. K., Scattering of Waves by Two-dimensional Circular Obstacles in Finite Water Depths, Journal of Ship Research, Vol. 23, Issue 1, 1979, pp. 32–42.
- [22] Raman H., Shankar J., and Dattatri J., Submerged Breakwaters, Central Board of Irrigation and Power Journal, Vol. 34, 1977, pp. 205–212.
- [23] Twu S. -W., Liu C. -C., and Hsu W. -H., Wave Damping Characteristics of Deeply Submerged Breakwaters. Journal of Waterway, Port, Coastal, and Ocean Engineering, Vol. 127, Issue 2, 2001, pp. 97–105.
- [24] Seelig W. N., Two-dimensional Tests of Wave Transmission and Reflection Characteristics of Laboratory Breakwaters, Technical Report of Coastal Engineering Research Center Fort Belvoir VA, No. 80-1, 1980.
- [25] Chen H. -B., Tsai C. -P., and Jeng C. -C., Wave Transformation between Submerged Breakwater and Seawall, Journal of Coastal Research, 2007.
- [26] Hajivalie F., The Effect of Submerged Breakwater Shape and Size on Wave Energy Dissipation, in Proceeding of the 37th IAHR World Congress, Vol. 6, 2017, pp. 3855-3860.
- [27] Pudjaprasetya S. and Magdalena I., Momentum Conservative Schemes for Dam Break and Wave Run-up Simulation, East Asian Journal on Applied Mathematics, Vol. 4, Issue 2, 2014, pp. 152–165.

- [28] Magdalena I., Iryanto, and Reeve D. E., Free Surface Long Wave Propagation over Linear and Parabolic Transition Shelves, Water Science and Engineering, Vol. 11, Issue 4, 2019, pp. 318–327.
- [29] Magdalena I., Pudjaprasetya S. R., and Wiryanto L. H., Wave Interaction with Emerged Porous Structure, Advances in Applied Mathematics and Mechanics, Vol. 6, Issue 5, 2014, pp. 680–692.
- [30] Magdalena I. and Rif'atin H. Q., Analytical and Numerical Studies for Harbor Oscillation in a Semi-closed Basin of Various Geometric Shapes with Porous Media, Mathematics and Computers in Simulation, Vol. 170, 2020, pp. 351–365.
- [31] Magdalena I., Non-hydrostatic Model for Solitary Waves Passing Through a Porous

- Structure, Journal of Disaster Research, Vol. 11, 2016, pp. 957–963.
- [32] Magdalena I., Erwina N., and Pudjaprasetya S., Staggered Momentum Conservative Scheme for Radial Dam Break Simulation, Journal of Scientific Computating, Vol. 65, 2015, pp. 867–874.
- [33] Teng M. H. and Wu T. Y., Nonlinear Water Waves in Channels of Arbitrary Shape, Journal of Fluid Mechanics, Vol. 242, 1992, pp. 211-233.
- [34] Synolakis C. E., The Run-up of Solitary Waves, Journal of Fluid Mechanics, Vol. 185, 1987, pp. 523-545.

Copyright © Int. J. of GEOMATE. All rights reserved, including the making of copies unless permission is obtained from the copyright proprietors.